

A new method for sampled fiber Bragg grating fabrication by use of both femtosecond laser and CO₂ laser

Xia Fang, X. Y. He, C. R. Liao, Minwei Yang, D. N. Wang*, Ying Wang

*Department of Electrical Engineering, The Hong Kong Polytechnic University,
Hung Hom, Kowloon, Hong Kong, P. R. China*

**eednwang@polyu.edu.hk*

Abstract: A new method for sample fiber Bragg grating fabrication by use of both femtosecond laser and CO₂ laser has been proposed and demonstrated. Such a method exhibits the advantages of high fabrication flexibility, and good thermal stability. The sampling period and duty cycle can be easily varied by changing the CO₂ laser beam scanning pattern during operation. The gratings produced have potential applications in optical communications, fiber lasers, and optical fiber sensors.

©2010 Optical Society of America

OCIS codes: (060.3735) Fiber Bragg gratings; (230.4000) Microstructure fabrication; (320.7140) Ultrafast processes in fibers; (140.7090) Ultrafast lasers.

References and links

1. F. Ouellette, P. A. Krug, T. Stephens, G. Dhosi, and B. Eggleton, "Broadband and WDM dispersion compensation using chirped sampled fibre Bragg gratings," *Electron. Lett.* **31**(11), 899–901 (1995).
2. L. Hojoon, and G. P. Agrawal, "Add-drop multiplexers and interleavers with broad-band chromatic dispersion compensation based on purely phase-sampled fiber gratings," *IEEE Photon. Technol. Lett.* **16**(2), 635–637 (2004).
3. Y. Jianliang, T. Swee Chuan, and N. Nam Quoc, "Multiwavelength tunable fiber ring laser based on sampled chirp fiber Bragg grating," *IEEE Photon. Technol. Lett.* **16**(4), 1026–1028 (2004).
4. J. Chow, G. Town, B. Eggleton, M. Ibsen, K. Sugden, and I. Bennion, "Multiwavelength generation in an erbium-doped fiber laser using in-fiber comb filters," *IEEE Photon. Technol. Lett.* **8**(1), 60–62 (1996).
5. G. Bai-Ou, T. Hwa-Yaw, T. Xiao-Ming, and D. Xiao-Yi, "Simultaneous strain and temperature measurement using a superstructure fiber Bragg grating," *IEEE Photon. Technol. Lett.* **12**(6), 675–677 (2000).
6. O. Frazão, R. Romero, G. Rego, P. V. S. Marques, H. M. Salgado, and J. L. Santos, "Sampled fibre Bragg grating sensors for simultaneous strain and temperature measurement," *Electron. Lett.* **38**(14), 693–695 (2002).
7. X. Shu, B. A. L. Gwandu, Y. Liu, L. Zhang, and I. Bennion, "Sampled fiber Bragg grating for simultaneous refractive-index and temperature measurement," *Opt. Lett.* **26**(11), 774–776 (2001).
8. B. A. L. Gwandu, X. W. Shu, Y. Liu, W. Zhang, L. Zhang, and I. Bennion, "Simultaneous measurement of strain and curvature using superstructure fibre Bragg gratings," *Sens. Actuators A Phys.* **96**(2-3), 133–139 (2002).
9. A. Asseh, H. Storoy, B. E. Sahlgren, S. Sandgren, and R. A. H. Stubbe, "A writing technique for long fiber Bragg gratings with complex reflectivity profiles," *J. Lightwave Technol.* **15**(8), 1419–1423 (1997).
10. H. Chi, X.-M. Tao, D.-X. Yang, and K.-S. Chen, "Simultaneous measurement of axial strain, temperature, and transverse load by a superstructure fiber grating," *Opt. Lett.* **26**(24), 1949–1951 (2001).
11. K. M. Davis, K. Miura, N. Sugimoto, and K. Hirao, "Writing waveguides in glass with a femtosecond laser," *Opt. Lett.* **21**(21), 1729–1731 (1996).
12. D. D. Davis, T. K. Gaylord, E. N. Glytsis, S. G. Kosinski, S. C. Mettler, and A. M. Vengsarkar, "Long-period fibre grating fabrication with focused CO₂ laser pulses," *Electron. Lett.* **34**(3), 302–303 (1998).
13. Y.-P. Wang, D. N. Wang, W. Jin, Y.-J. Rao, and G.-D. Peng, "Asymmetric long period fiber gratings fabricated by use of CO₂ laser to carve periodic grooves on the optical fiber," *Appl. Phys. Lett.* **89**(15), 151105–151103 (2006).
14. H. Patrick, S. L. Gilbert, A. Lidgard, and M. D. Gallagher, "Annealing of Bragg gratings in hydrogen-loaded optical fiber," *J. Appl. Phys.* **78**(5), 2940–2945 (1995).
15. G. Bai-Ou, T. Hwa-Yaw, T. Xiao-Ming, and D. Xiao-Yi, "Highly stable fiber Bragg gratings written in hydrogen-loaded fiber," *IEEE Photon. Technol. Lett.* **12**(10), 1349–1351 (2000).
16. A. L. C. Triques, C. L. Barbosa, and R. M. Cazo, "J. L. de, S. Ferreira, R. C. Rabelo, L. C. G. Valente, A. Martins, and B. Braga, "Thermal treatment of fiber Bragg gratings recorded using high power lasers," *J. Microwaves and Optoelectronics* **3**, 127–134 (2004).
17. Y. Li, C. R. Liao, D. N. Wang, T. Sun, and K. T. V. Grattan, "Study of spectral and annealing properties of fiber Bragg gratings written in H₂-free and H₂-loaded fibers by use of femtosecond laser pulses," *Opt. Express* **16**(26), 21239–21247 (2008).

18. S. J. Mihailov, C. W. Smelser, P. Lu, R. B. Walker, D. Grobnic, H. Ding, G. Henderson, and J. Unruh, "Fiber bragg gratings made with a phase mask and 800-nm femtosecond radiation," *Opt. Lett.* **28**(12), 995–997 (2003).
 19. A. J. C. Grellier, N. K. Zayer, and C. N. Pannell, "Heat transfer modelling in CO₂ laser processing of optical fibres," *Opt. Commun.* **152**(4-6), 324–328 (1998).
 20. T. Erdogan, "Fiber grating spectra," *J. Lightwave Technol.* **15**(8), 1277–1294 (1997).
 21. X. Y. He, Y. L. Yu, D. X. Huang, R. K. Zhang, W. Liu, and S. Jiang, "Analysis and applications of reflection-spectrum envelopes for sampled gratings," *J. Lightwave Technol.* **26**(6), 720–728 (2008).
-

1. Introduction

Sampled fiber Bragg grating (SFBG) has many attractive applications in optical communications [1,2], multi-wavelength fiber lasers [3,4], and optical fiber sensors [5–8]. It is usually fabricated by use of UV light irradiation on hydrogenated single mode fiber (SMF) and the amplitude or phase of its reflection spectrum is modulated by a sampling function. Such a modulation can be achieved by periodically triggering on and off the light exposure along the fiber [7,8], which needs an accurate control of the light exposure time, power and location for each subgrating, and the apolization is obtained by multiple exposures with different power levels for different subgrating sections [9]. Alternatively, a specially designed amplitude mask can be employed together with the phase mask during the grating inscription process however, owing to the fixed modulation envelope, different amplitude masks have to be used to produce different modulation profiles [5,10].

In this paper, we propose an SFBG fabrication method by use of both femtosecond laser and CO₂ laser, which allows the modulation envelop to be flexibly changed according to the application requirement. Because of the multi-photon absorption [11] of the femtosecond laser inscription and the CO₂ laser heating effect [12,13], SFBG can be created in SMF without hydrogen loading. The temperature test reveals that the SFBGs fabricated in this work have a good thermal stability up to 650 °C, superior to those fabricated in hydrogen loaded SMF by UV light without special treatment that begin to decay significantly at temperatures between 100 to 200 °C [14–16].

2. SFBG fabrication and theoretical background

2.1 SFBG fabrication method

A femtosecond laser and a CO₂ laser are both used to fabricate the SFBG with flexible control of its reflection peaks and the peak spacing. The whole fabrication process is divided into two stages. First, a fiber Bragg grating (FBG) is inscribed in SMF using femtosecond laser pulses through a phase mask [17], which is initially demonstrated in [18]. The femtosecond laser pulses (120 fs, 1 mJ, 1 kHz repetition rate at $\lambda = 800$ nm) are produced by a Ti: Sapphire laser system (Spectra-Physics). The laser pulse energy could be adjusted as required by rotating a half wave-plate followed with a linear polarizer and the energy of ~0.6 mJ was used during the grating fabrication. The laser beam is broadened through a laser beam expander which is used to tune the laser spot size, and then focused by a cylindrical lens with a focal length of 60 mm before passing through a silica phase mask (Ibsen Photonics) and arriving at the fiber core. The position of the fiber is accurately controlled by a high-precision four-axis translation stage. By use of appropriate laser exposure condition, the FBG with predetermined length can be produced. The length of FBG can be varied from 4 to 12 mm by tuning the laser beam expander. By considering the effects of both the laser intensity and the quality of the reflection spectrum, the FBG length of 8 mm is chosen in our experiment.

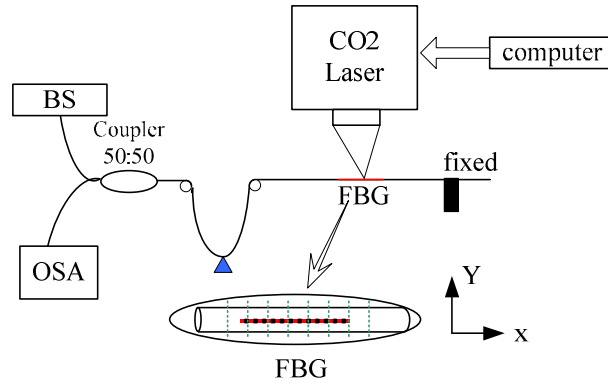


Fig. 1. Experimental arrangement for SFBG fabrication by CO₂ laser scanning. BS denotes the broadband light source. The green dotted lines indicate the scanning route of the CO₂ laser beam and the red line with block dots indicates the FBG.

The second stage is to use a high frequency CO₂ laser (SYNRAD 48-1) for reprocessing the FBG obtained. The experimental set-up is demonstrated in Fig. 1. The CO₂ laser beam is focused onto the fiber with FBG, which is mounted on a translation stage. One end of the FBG is fixed and the other is dragged by a small weight of ~5 g to avoid any induced micro-bend of the fiber during the laser heating process. The average power of the focused CO₂ laser light is ~0.5 W with a repetition frequency of 10 kHz, and a diameter of ~50 μm. By use of a computer controlled two-dimensional optical scanner with the spatial resolution of 1 μm, the CO₂ laser beam scans and shifts along the green dotted lines as shown in Fig. 1, which are perpendicular to the X direction along the fiber length. After one scanning cycle, the laser beam is moved to the first green dotted line again and repeats the scanning process. Such a scanning process continuous until the designed pattern for the sampled grating structure is obtained. A broadband light source (AMONICS ALS-SWDM-FA) and an optical spectrum analyzer (OSA) with resolution of 0.01 nm are used to monitor the reflection spectrum of the grating during the fabrication process.

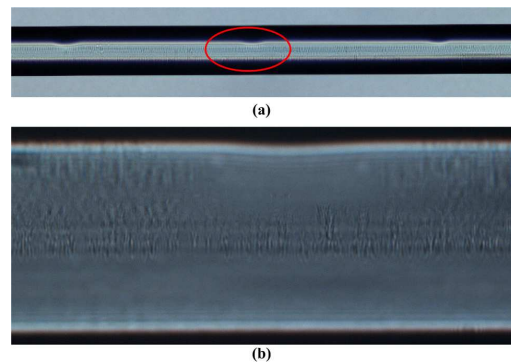


Fig. 2. (a) Microscope image of the SFBG fabricated by femtomsecond laser and CO₂ laser. (b) The amplified image of the part circled in (a).

Figure 2(a) shows a microscope (Nikon 80i) image of the SFBG structure created. An amplified image that provides more details is shown in Fig. 2(b). The grooves carved on the fiber are caused by the CO₂ laser heating [19], which imposes a periodic index modulation on the reflection spectrum of the FBG inscribed by femtosecond laser.

2.2 Theoretical background of the SFBG fabricated

A normal FBG has an effective refractive index distribution as shown in Fig. 3(a). When a periodic modulation of the effective refractive index is introduced to the FBG as shown in

Fig. 3(b), an SFBG is created and its index profile is shown in Fig. 3(c), which can be described by:

$$n_{eff}(z) = n_{0,eff}(z) + \bar{\delta}n_{eff}(z) \cdot \left[f(z) * \left(\sum_{i=-\infty}^{\infty} \delta(z - iZ_0) \cdot g(z) \right) \right] \cdot \left\{ 1 + \nu \cos\left(\frac{2\pi}{\Lambda} z\right) \right\} \quad (1)$$

$$f(z) = \begin{cases} 1, & -\frac{Z_g}{2} \leq z \leq \frac{Z_g}{2} \\ 0, & \text{otherwise} \end{cases} \quad (2)$$

$$g(z) = \begin{cases} \exp\left(\frac{-4 \ln 2 z^2}{W^2}\right), & -\frac{L_0}{2} \leq z \leq \frac{L_0}{2} \\ 0, & \text{otherwise} \end{cases} \quad (3)$$

where $n_{0,eff}$ is the average effective refractive index for the propagating mode, $\bar{\delta}n_{eff}$ is the dc index change spatially averaged over a grating, ν is the fringe visibility of the index change, Λ is the grating period, Z_0 and Z_g are the sampling period and the grating segment length of the sampling period, respectively. L_0 is the total length of the conventional SFBG and W is the full-width-at-half-maximum value of the grating profile, which is equal to $L_0/2$ in our modeling. The rectangular function $f(z)$ is the sampling function of the SFBG without apodization, and the function $g(z)$ is the whole grating profile function with Gaussian apodization, which is used to simulate the Gaussian intensity profile of the femtosecond laser beam.

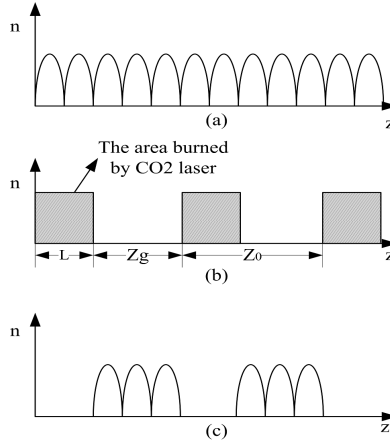


Fig. 3. (a) Effective refractive index profile of the FBG. (b) CO₂ laser induced periodic modulation. (c) Effective refractive index profile of the SFBG.

According to the Transfer Matrix Method [20], we can simulate the SFBG by subdividing the grating structure into multiple sections, each of which can be identified by a 2×2 matrix. For the sake of simplicity, the area with grating structure exposed by the light of the CO₂ laser is treated as a pure phase section, because the high temperature produced by the CO₂ laser beam can diminish the grating structure as shown in Fig. 2. The grating section exposed to the CO₂ laser light can be expressed by the matrix:

$$F = \begin{bmatrix} e^{j\beta L} & 0 \\ 0 & e^{-j\beta L} \end{bmatrix} \quad (4)$$

where L is the length of exposed areas in one period as shown in Fig. 3 (b), $\beta = \frac{2\pi n_{\text{eff}}}{\lambda}$ is the propagation constant, and λ is the light wavelength.

The unexposed area to the CO₂ laser light in the FBG is still a normal Bragg grating and is divided into a number of uniform sections, each section is described by:

$$T_{p,n} = \begin{bmatrix} \cosh(\gamma Z_g) - j \frac{\sigma}{\gamma} \sinh(\gamma \Delta z) & -j \frac{\kappa}{\gamma} \sinh(\gamma \Delta z) \\ j \frac{\kappa}{\gamma} \sinh(\gamma \Delta z) & \cosh(\gamma Z_g) + j \frac{\sigma}{\gamma} \sinh(\Delta z) \end{bmatrix} \quad (5)$$

where $T_{p,n}$ denotes the n th uniform section in the p th unexposed region of the SFBG, Δz is the section length, κ is the AC coupling coefficient, $\gamma = \sqrt{\kappa^2 - \sigma^2}$, and σ is the DC coupling coefficient. Thus, the p th unexposed region of the SFBG can be expressed by the matrix:

$$T_p = T_{p,m} \cdot T_{p,m-1} \cdots T_{p,2} T_{p,0} \quad (6)$$

where, m denotes the total number of the uniform sections in one unexposed area. Then the SFBG can be described by:

$$T = T_q F T_{q-1} \cdots T_2 F T_1 \quad (7)$$

where, q represents the total number of the unexposed region in the SFBG. It becomes clear that the reflection spectrum can be obtained from Eqs. (1) to (7), by use of transfer matrix method [20].

3. Experimental and simulation results and discussion

The inset picture of Fig. 4 shows the reflection spectrum of the FBG fabricated by femtosecond laser in our experiment. The grating has a 3dB bandwidth of around 0.5 nm and center wavelength of ~1569 nm. In the second stage of SFBG fabrication process, the CO₂ laser beam is scanned along the FBG in 40 parallel lines with a separation of 450 μm , being perpendicular to the X direction of the fiber as shown in Fig. 1. The scanning line has a length of 1 mm, which ensures that the laser crosses the whole fiber. The laser scanning speed is set as 3.57 mm/s, which results in a power density of 2.8 J/mm² on the fiber surface, and the scanning time is approximately 0.3 s for each dotted lines. After only one sweep of the CO₂ laser, the side peaks appear in the reflection spectrum of the SFBG as demonstrated in Fig. 4. The intensity of the center peak is reduced by 3.9 dB, and the wavelength experiences a blue shift of ~0.21 nm compared with the original spectrum of the FBG. Figure 5 shows the evolution of the reflection spectrum corresponding to the different number of sweep cycles. When the intensity of the center peak is decreased with the increase of the number of sweep cycles, the intensity of the side peak is increased. After the five sweep cycles, the blue shift of the center wavelength is 0.38 nm and its intensity is reduced by 6.65 dB compared with the original FBG spectrum. However, the amount of shifted wavelength and the intensity change in each scanning cycle decrease with the increase of the number of sweep cycles. The blue shift of wavelength is likely due to the average refractive index decrease of the FBG during the CO₂ laser beam scanning process. With the number of sweep cycles increases, such an effect is intensified and the blue shift is enhanced. The envelop of SFBG is mainly determined by Z_g when the sampling period is a constant [21]. The increase of the number of the scanning cycles will essentially enhance the energy on the periphery of the CO₂ laser spot and resulting in the shortening of grating segment length. Thus, the increase of the number of

scanning cycles leads to a broad envelop of the SFBG and low reflectivity value of the center peak. However, the spacing of the adjacent peaks remains to be ~ 1.87 nm, owing to the constant sampling period of the grating.

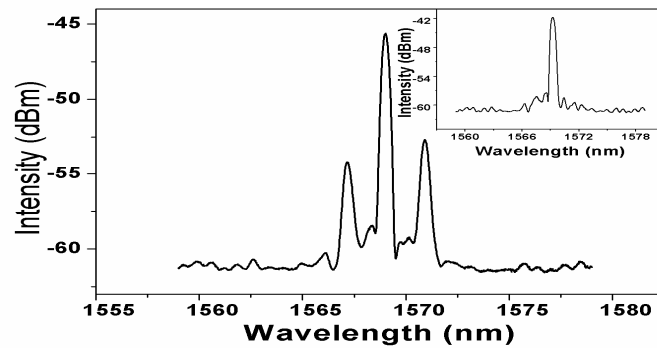


Fig. 4. Reflection spectrum of the SFBG corresponding to one laser scanning cycle. The insert picture shows the original reflection spectrum of FBG fabricated by femtosecond laser.

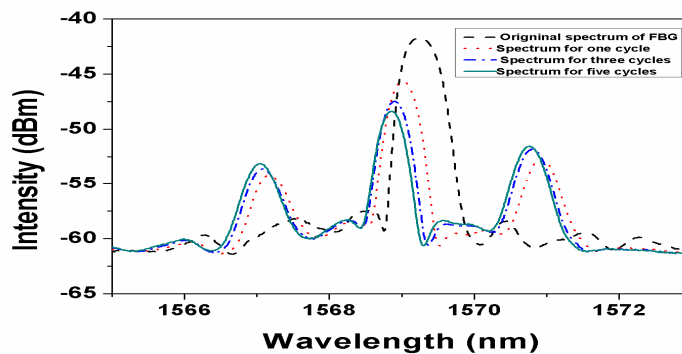


Fig. 5. Reflection spectra of the SFBG corresponding to 1, 3, and 5 laser scanning cycles.

The reflection peak spacing is inversely proportional to the spacing of the CO₂ laser scanning line, which is denoted by Z_0 in simulation. When the scanning line spacing is set to be 300, 400, and 450 μm , the corresponding peak spacing obtained is 2.8, 2.1 and 1.87 nm, which is in good agreement with the value obtained in the simulations, i.e. 2.78, 2.11, and 1.87 nm, respectively. Thus, the spacing of the adjacent peaks is mainly determined by the sampling period as shown in Fig. 6.

The intensity differences appear in Fig. 6(a)-(c) are caused by the variation of the output power from the broadband source, the connection loss between FBG and coupler and the fiber end face reflection, etc, in different experimental conditions. Moreover, the power of CO₂ laser also introduces fluctuation. The higher the CO₂ laser intensity, the larger the erased part of the grating, and the lower the reflectivity of the SFBG obtained. The intensities of the side-lobes shown in Fig. 6(d), (e), (f) are below -80dBm and cannot be detected by the OSA used, which has a resolution of -75dBm . The intensity difference between simulation and experimental results is caused by the OSA sensitivity, coupler inherent reflection, and reflections from fiber connectors and end faces.

The duty ratio (DR) of the sampled grating, which is defined as the ratio of Z_g to Z_0 , has a great effect on the number of peaks. The method of realizing a certain duty ratio in the experiment is that after each sweep cycle of the CO₂ laser, the scanning line is shifted by 30 μm along the X direction. The process continuous until a certain duty ratio is obtained. The duty ratio after each scanning cycle can be calculated by the equation as below:

$$DR = 1 - \frac{30\mu m \times (N - 1) + 50\mu m}{Z_0} \quad (8)$$

where N is the number of scanning cycle, the displacement of the parallel line is $30\ \mu\text{m}$ and the diameter of the CO_2 spot is $50\ \mu\text{m}$. In Fig. 7, the sampling period of the SFBG used is $400\ \mu\text{m}$, and the duty ratios are 0.88, 0.65 and 0.425, respectively, corresponding to 1, 4 and 7 scanning cycles, respectively, according to Eq. (8). As shown in Fig. 7(a), there are only three peaks after one sweep cycle, and the number of the peaks is increased to four after four sweep cycles. The peaks number reaches five when the DR is 0.575. When the scanning cycle increases, the intensity of the center peak reduces and the envelope of the spectrum becomes flat, caused by the shortening of grating segment length as discussed above. The experimental results obtained in Fig. 7(a) have a good agreement with those obtained in the simulations as shown in Fig. 7(b).

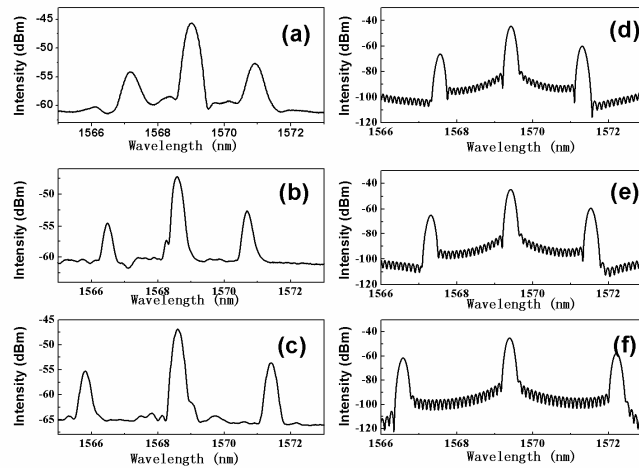


Fig. 6. Experimental results for the sampling period of (a) $450\ \mu\text{m}$, (b) $400\ \mu\text{m}$, and (c) $300\ \mu\text{m}$. Simulation results for the sampling period of (d) $450\ \mu\text{m}$, (e) $400\ \mu\text{m}$, and (f) $300\ \mu\text{m}$.

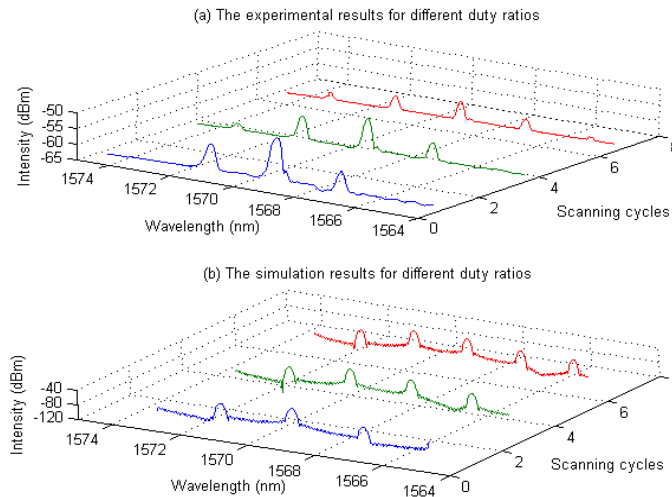


Fig. 7. (a) Experimental results of the SFBG reflection spectra for different duty ratios: 0.88 (one scanning cycle), 0.65 (four scanning cycles) and 0.425 (seven scanning cycles). (b) The corresponding simulation results.

The behavior of the SFBG that changes with the temperature has also been investigated. The SFBG is placed in the tube furnace, and its center reflection peak is monitored by use of an OSA. The temperature was increased by a step of 50 °C, and was maintained for 10 minutes at each step. No significant decrease of the center peak was found up to 600 °C, as shown in Fig. 8. When the temperature is further increased to 700 °C, the peak intensity started to decrease rapidly. After being maintained at 700 °C for about 20 minutes, the temperature was decreased to 650 °C, where the center peak was found to become stable again. The temperature was then decreased to the room temperature and the center peak intensity was stable in the whole cooling process.

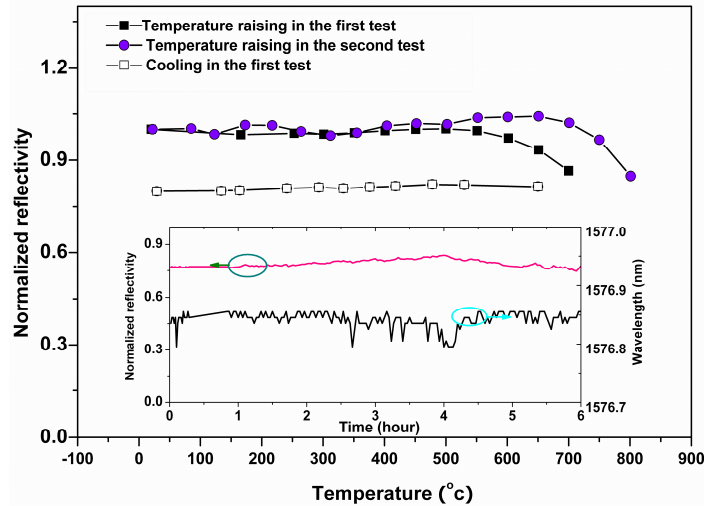


Fig. 8. SFBG peak intensity versus temperature. The inset shows the result of thermal stability test at 650°C for six hours.

When the temperature was increased again, the center peak intensity did not decrease significantly until at 700 °C. This is likely due to the fact that the unstable factors have been removed in the first thermal test. When the temperature reached 800 °C, there was still more than 80% power remaining compared with that at room temperature when the second test started. A good thermal stability maintained when the temperature was kept at 650 °C for six hours.

The thermal stability can be further improved by using a larger exposure power and a longer exposure time in the manufacturing process [17], the former can induce a permanent local structure damage. However, it also creates the difficulty in erasing the refractive index modulation by the CO₂ laser to form a pure phase section in the FBG. The purity of the phase section has a significant effect on the spectral quality of the SFBG, and a reduced erasing capability of the CO₂ laser will result in a poor spectral quality of the SFBG. Thus, a balance between the spectral quality and the thermal stability should be established, depending on the type of applications.

4. Conclusion

We have proposed a new method for SFBG fabrication in conventional SMF without hydrogen loading, in which the sampling period and the duty ratio can be easily controlled and as a result, the reflection spectrum of the grating can be flexibly modulated by just varying the CO₂ laser scanning route. The use of both femtosecond laser and CO₂ laser can also effectively enhance the thermal stability of the grating. The SFBG developed in this work have high potential in fiber laser and optical fiber sensor applications.

Acknowledgment

This work was supported by the Hong Kong SAR government through a GRF grant PolyU 5291/07E and the Hong Kong Polytechnic University research grant G-U501.